

Modeling and Fuzzy Logic Control of PV Based Cascaded Boost Converter Three Phase Five-level Inverter System

Guruswamy Revana, Venkata Reddy Kota

Department of Electrical and Electronics Engineering, Jawaharlal Nehru Technological University Kakinada, India

Article Info

Article history:

Received Apr 8, 2017

Revised Jul 10, 2017

Accepted Aug 1, 2017

Keyword:

Boost converter
Multi-level Inverter
PI controller
Solar panel

ABSTRACT

Power Quality development using PV based boost cascaded inverter system is one of the reliable methods. This paper handle with modeling and fuzzy logic control of boost to boost cascaded three phase inverter system with PV as source. MATLAB simulink model for BBCIS has been developed using the elements of simulink and cascaded loop investigations are performed with PI and Fuzzy Logic Controllers. The dynamic responses of the above systems are compared in terms of time domain parameters. The consequences point to that maximum power is obtained with minimum THD using FLC.

*Copyright ©2017 Institute of Advanced Engineering and Science.
All rights reserved.*

Corresponding Author:

Guruswamy Revana,
Department of Electrical and Electronics Engineering,
Jawaharlal Nehru Technological University Kakinada,
Kakinada, Andhra Pradesh, India.
Email: guru_revana@yahoo.com

1. INTRODUCTION

Due to privileged efficiency and slighter size, photovoltaic (PV) inverters without isolation transformers become more attractive in grid-connected PV systems [1]–[4]. Besides, generally they are not to routinely decrease DC current injection [5], which causes the saturation of distribution transformers in the grid and results in bad power quality, higher loss, Over heating in the power system [1], [6]. As a result, standards and regulations have been formulated to limit PV inverter DC injection to the grid. To decrease DC injection, some control methods have been proposed [1], [6], [7]. The methods of DC current booster repression can be mainly classified into four categories: blocking DC current with the capacitor, novel inverter configuration with DC current suppression capability, current-detection manages and voltage-detection organizes. The process of overcrowding DC current with the capacitor uses a serially connected capacitor between the inverter and the grid [12]. It requires a bulky and expensive capacitor and may cause extra loss. Guo et al developed a method to block DC current by using a virtual capacitor; however, the dynamic response of the closed-loop control system was affected by the virtual capacitor. The method of applying inverter topology with DC current suppression ability uses inherent structure of the inverter topology which can prevent DC current from injecting into the grid, e.g., the half-bridge inverter [13]. However, few practical topologies exist.

The way of current-detection control uses current sensors to find the DC current booster to the grid, but its effectiveness is limited by the accuracy of sensor due to the inherent zero-drift characteristic of Hall-effect current sensors. To solve the zero drift problems, an auto-calibrating inverter has been proposed by Armstrong [14]. However, this method requires determining the switching state of the H-bridge in order to measure the inherent zero-drift of the system. Sharma first detected a method of DC offset voltage. The grid current was removed by feeding back the DC offset voltage to the PI controller. DC offset detected at the

output of the low-pass filter is fed back to the controller. A mathematical model is presented in this paper. However, the experimental results under grid mode were not given. The voltage-detection control method uses sensors to detect the DC voltage offset across the ripple filter [15]. This method indicates that low DC voltage across the filter can be measured, which is sensitive to noise. A DC offset detection method is proposed by Buticchi [16]. However, this method needs a nonlinear inductor. Hence, a customized inductor should be designed according to specific systems. He and Xu [17] used a voltage sensor at the output of the inverter which consists of a differential amplifier and a low-pass filter. Alfock and Bowtell [19] continued studying this method by establishing the mathematical model and verified it.

The above literature does not deal with BBCIS based PV system with MPPT. This work deals with FLC based MPPT for BBCIS systems. This paper is organized as follows: Section II describes the details of proposed system. Section III analyzes the results of BBCIS with and without MPPT. Section IV provides experimental results to verify the theoretical analysis the conclusion is given in Section V.

2. PROPOSED SYSTEM

The block diagram of existing system is shown in Figure 1. The output of PV is stepped up using boost converter. The output of three phase inverter is employed on to the load. The block diagram of proposed system is shown in Figure 2. Two boost converters are cascaded to increase the voltage gain. The FLC is proposed to improve the dynamic response.

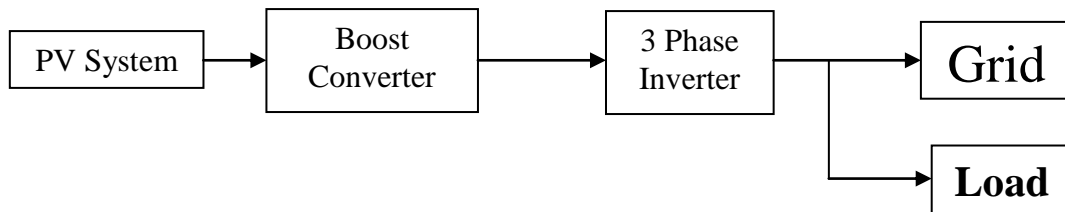


Figure 1. Block diagram of existing system

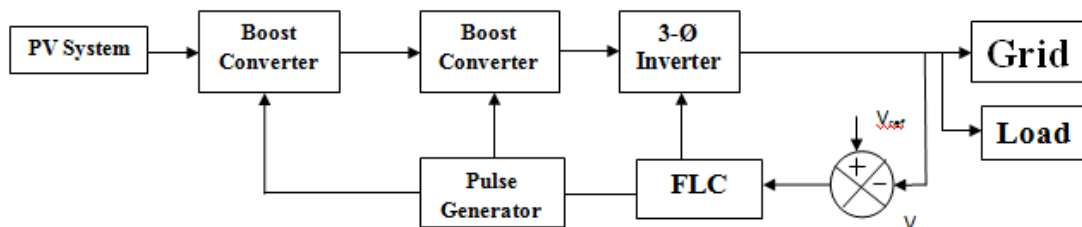


Figure 2. Block diagram of proposed system

3. SIMULATION RESULTS

PV inverter system with cascaded boost converter is shown in Figure 3. Scopes are connected to measure voltage, current and power. The output of PV system is boosted using two boost converters. The DC output is converted into AC using three phase inverter. The change in voltage due to reduction in light intensity is shown in Figure 4. The voltage reduces from 48 to 44 volts. The output voltage of boost converter is shown in Figure 5. The output voltage reduces from 190 to 170 volts. The switching pulses for M_2 , M_4 and M_5 are shown in Figure 7. PWM pulses are applied to the Switches. The phase current waveforms are shown in Figure 8. The load current is smoothed by the load inductance. The output power reduces from 230W to 190W as shown in Figure 9. The frequency spectrum for current is shown in Figure 10 and the THD is 10.1%. Lowest frequency is 50Hz and highest frequency is 900Hz. Fundamental component of current is 3.5A. Fifth harmonic is predominant and other harmonics are negligible.

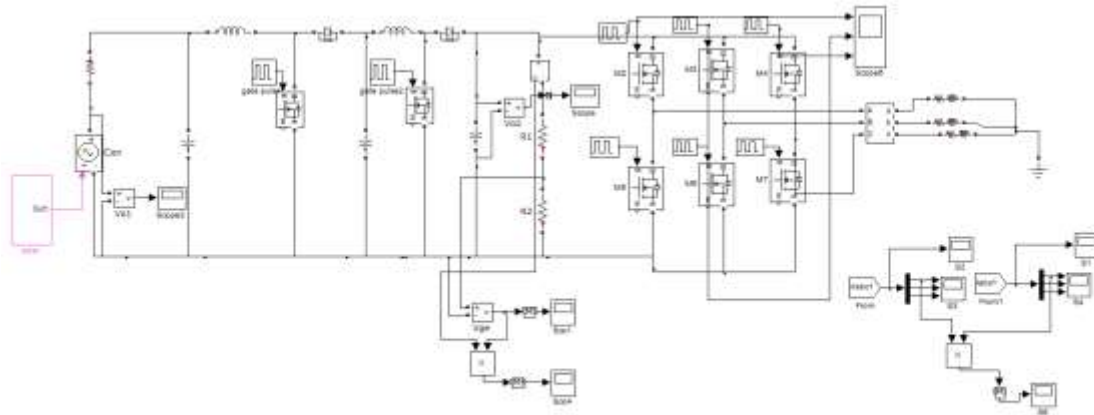


Figure 3. Circuit diagram for BBCIS without MPPT

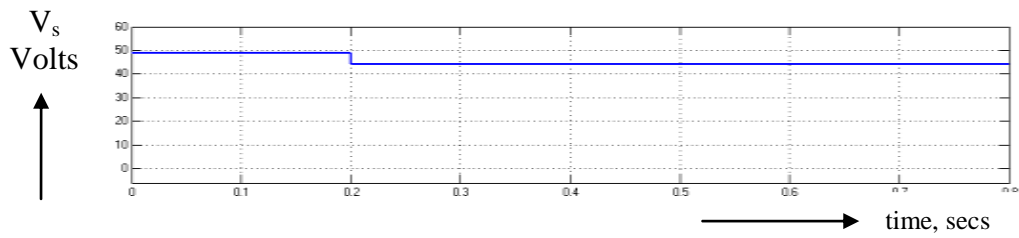


Figure 4. Output voltage of Solar System

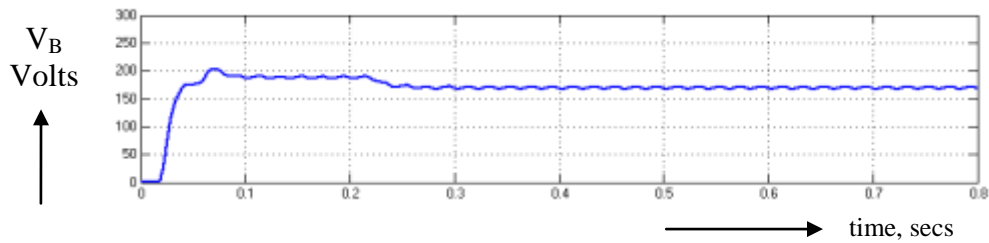


Figure 5. Output voltage of Boost to boost converter

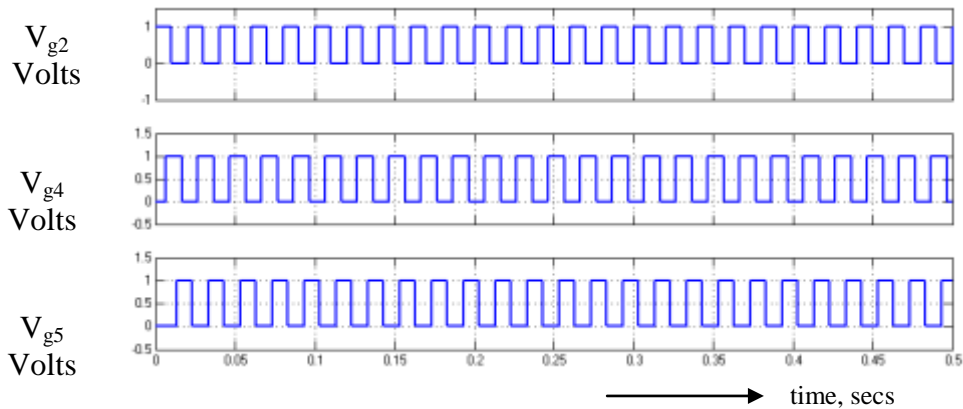


Figure 6. Switching pulses for S_1 , S_3 and S_5 inverter

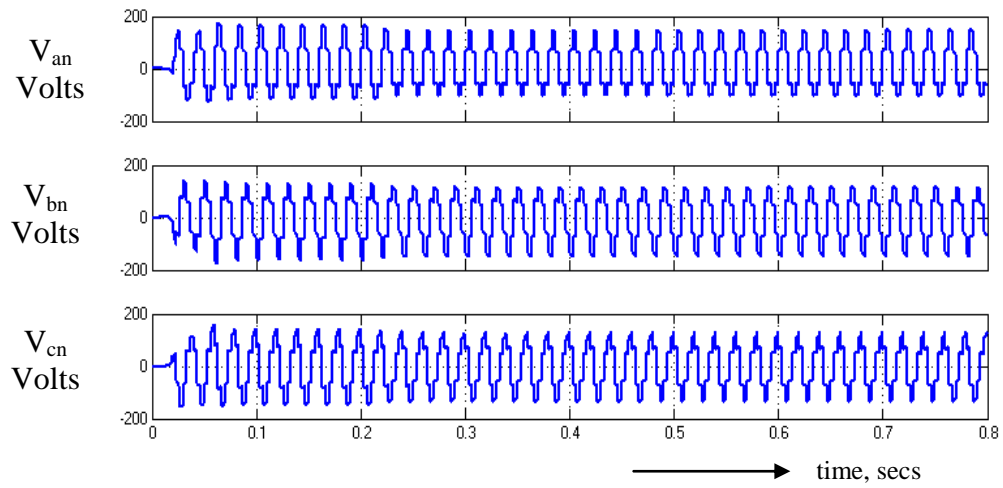


Figure 7. Output voltage waveforms

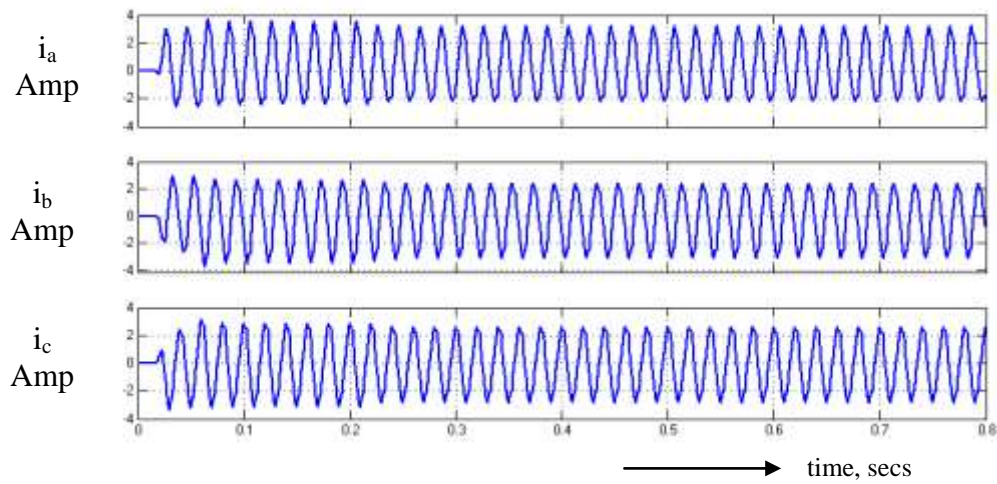


Figure 8. Output current waveforms

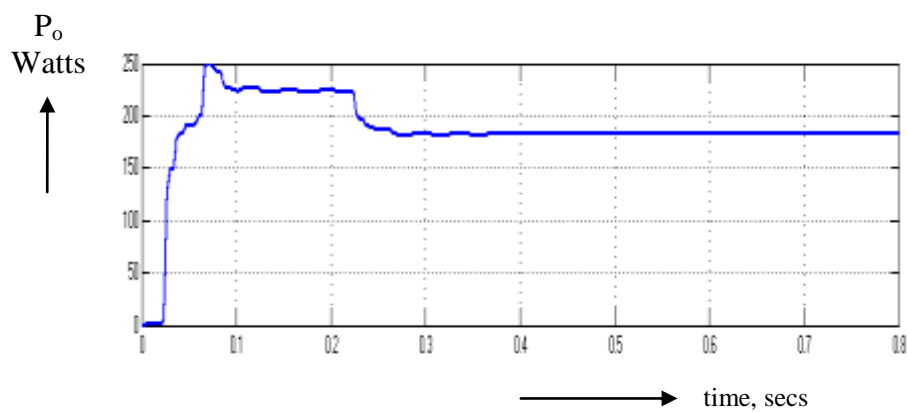


Figure 9. Output power

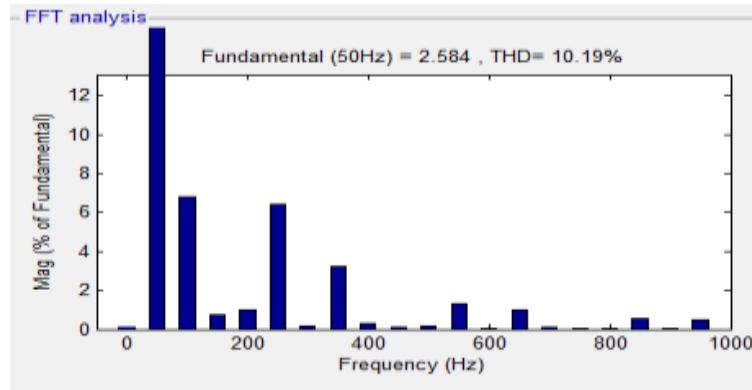


Figure 10. Frequency spectrum for the current

Closed loop PI controlled system with MPPT is shown in Figure 11. Actual power is measured and it is compared with reference power and the error is applied to PI controller. The output of PI controller is used to generate the pulses for the switches of the boost converter. The output of PV system is shown in Figure 12. The output of BC is shown in Figure 13. The output voltage is brought back to normal value. The three phase output voltages are shown in Figure 14. The three phase currents are depicted in Figure 15. The power output is shown in Figure 16 and it is maintained constant at 230W. The frequency spectrum for the current is shown in Figure 17 and the THD is 8.1%. Fundamental component of current is 2.58A. Fifth & seventh harmonics are predominant and other harmonics are negligible.

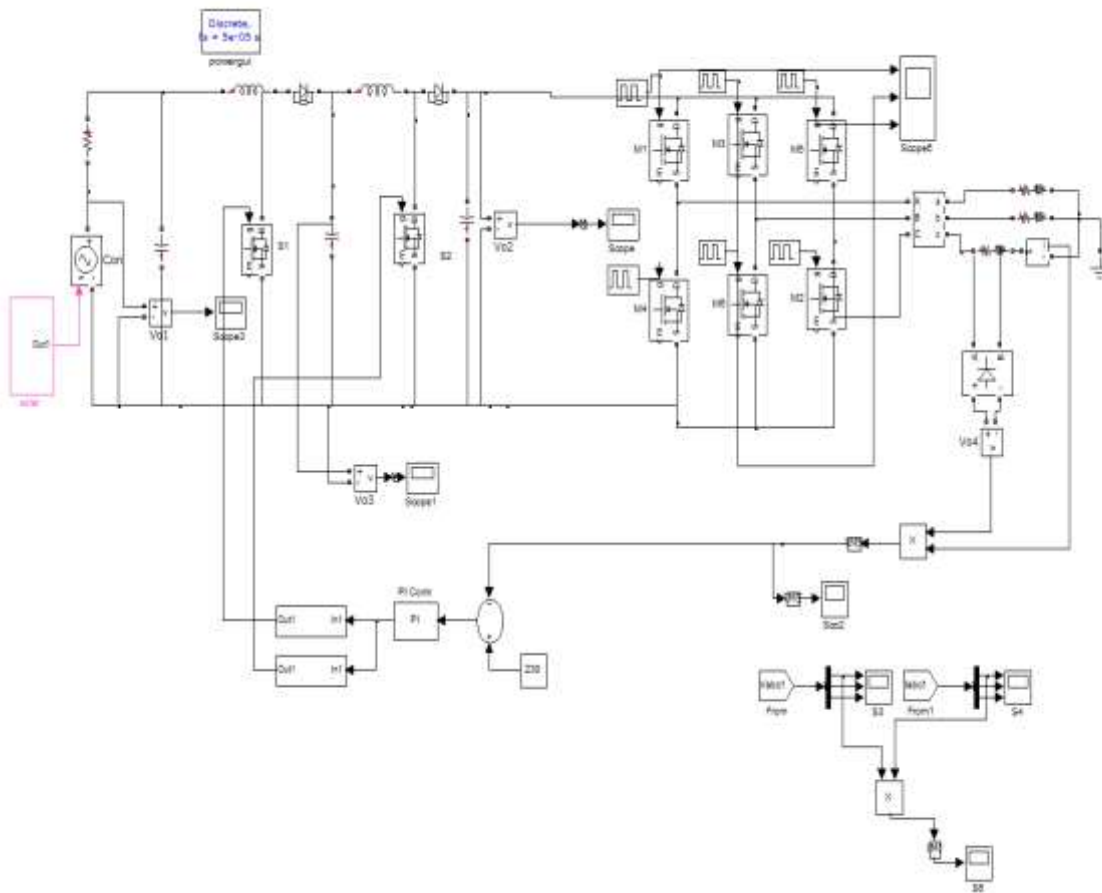


Figure 11. Circuit of BBCIS with MPPT and PI controller

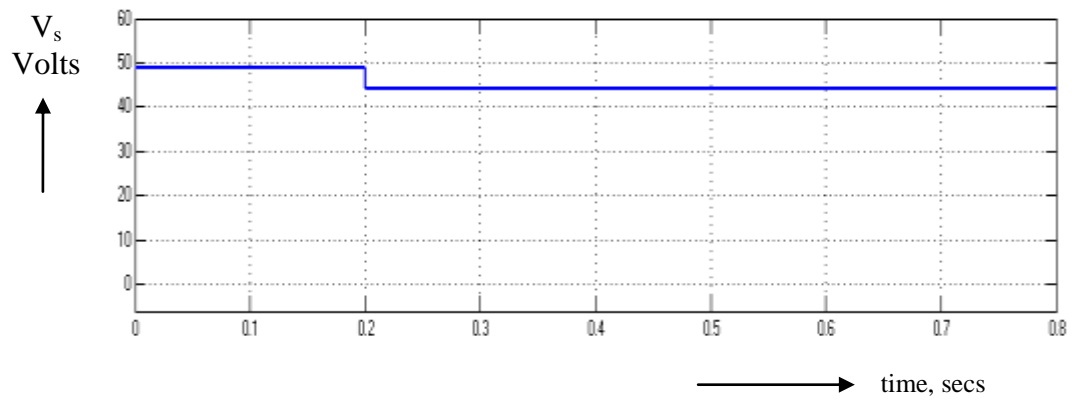


Figure 12. Output voltage of Solar System

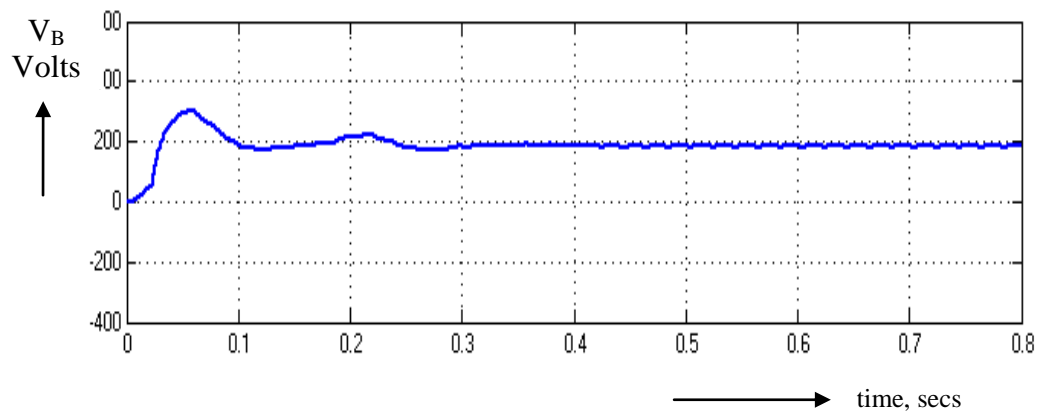


Figure 13. Output voltage of boost to boost converter

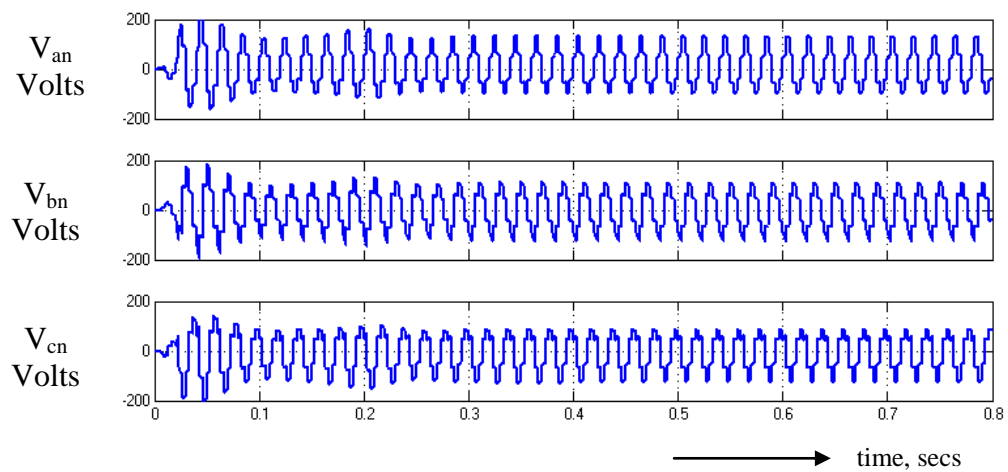


Figure 14. Output voltage waveforms of Inverter

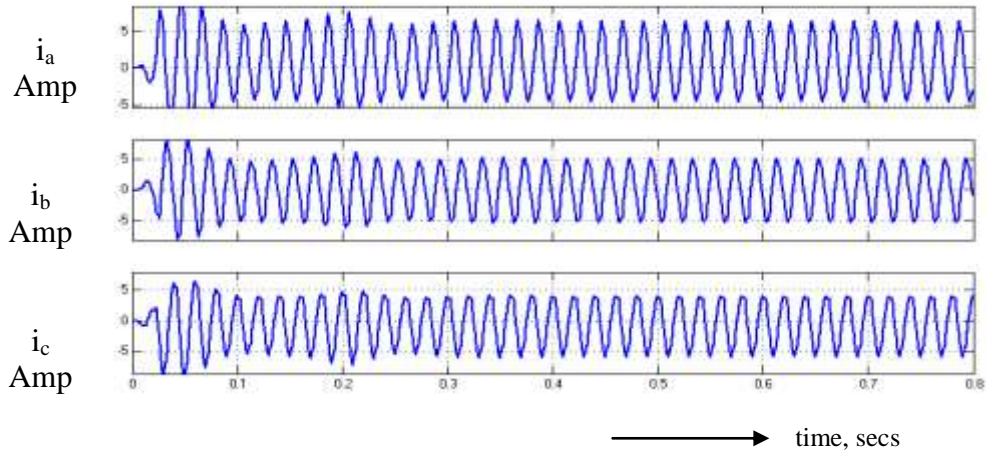


Figure 15. Load current waveforms

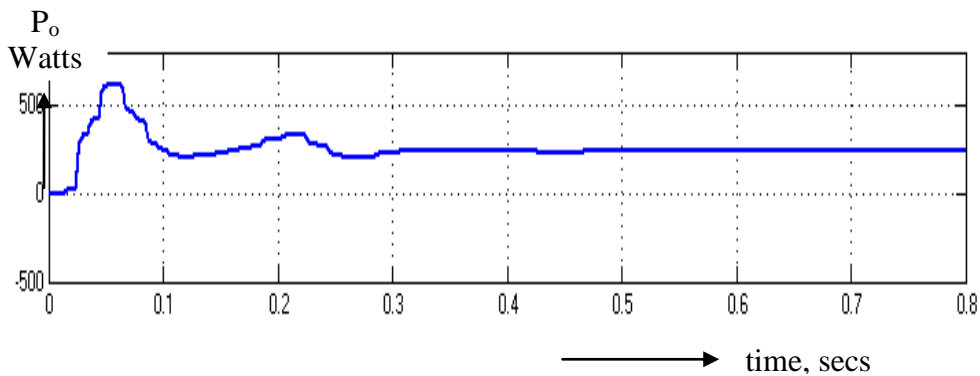


Figure 16. Output power

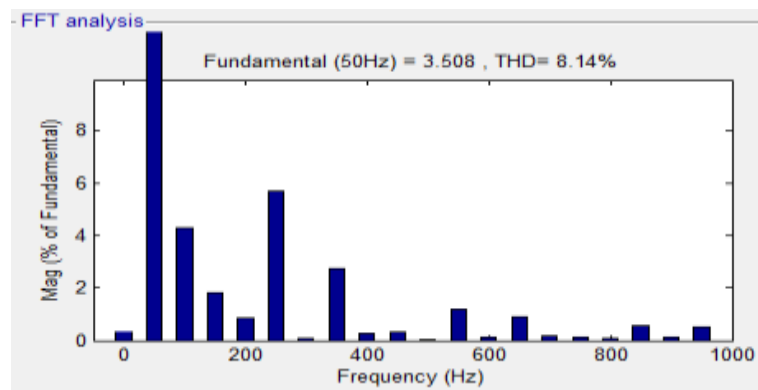


Figure 17. Frequency Spectrum for Load Current

The closed loop system with FLC is shown in Figure 18. The PI controller is substituted by FLC. The step reduction in voltage is shown in Figure 19. The output voltage of boost to boost converter is shown in Figure 20. The output voltage has settled at 200V. The three phase voltage and current waveforms of BBCIS are shown in Figures 21 and 22 respectively. The output power is shown in Figure 23 and is equal to 230W. The frequency spectrum for the current is shown in Figure 24 and the THD is reduced to 5.67%. The magnitude of fifth harmonic is 5.5% and the magnitude of seventh harmonic is 3%.

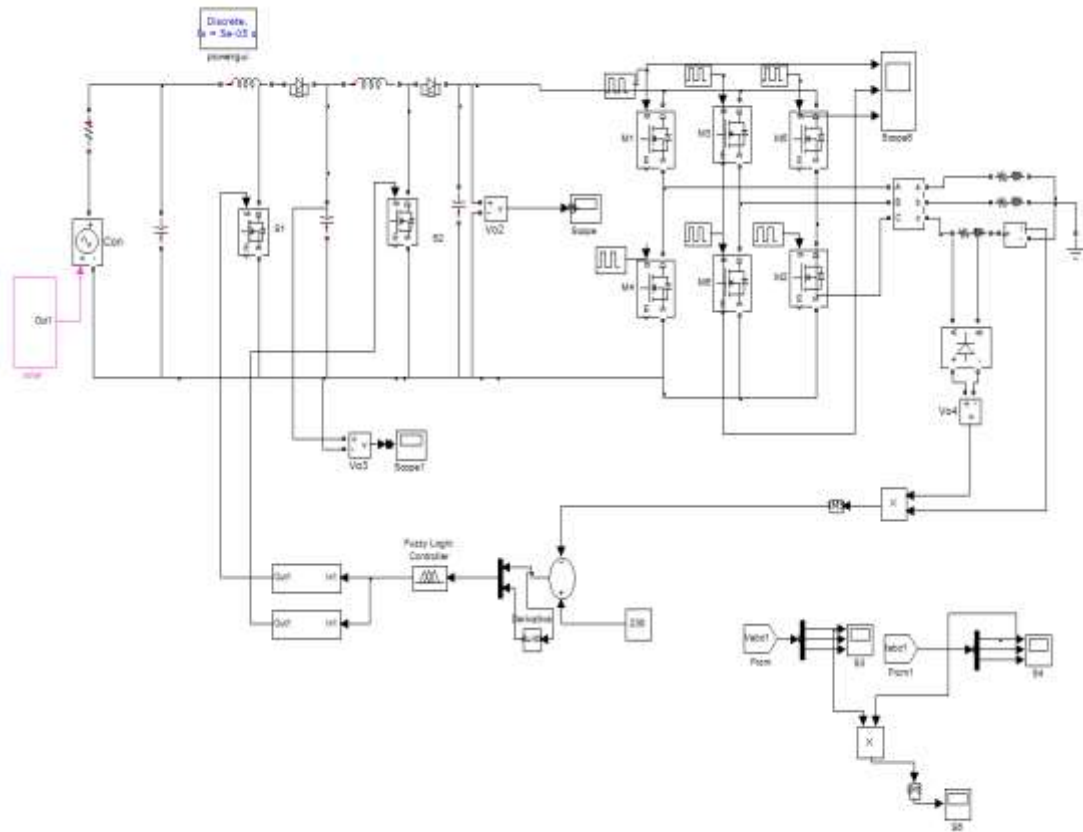


Figure 18. Circuit of BBCIS with MPPT using FLC

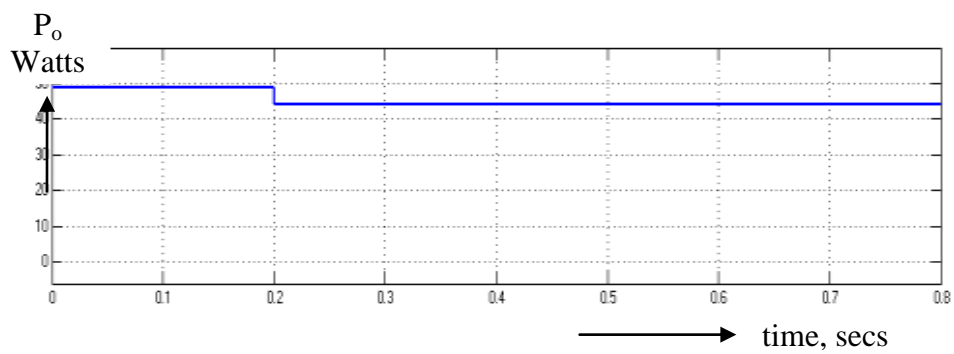


Figure 19. Output voltage of solar system

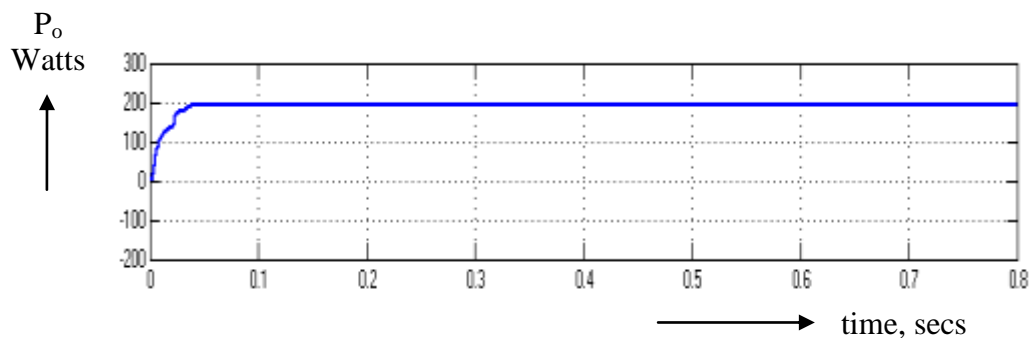


Figure 20. Output voltage of boost to boost converter

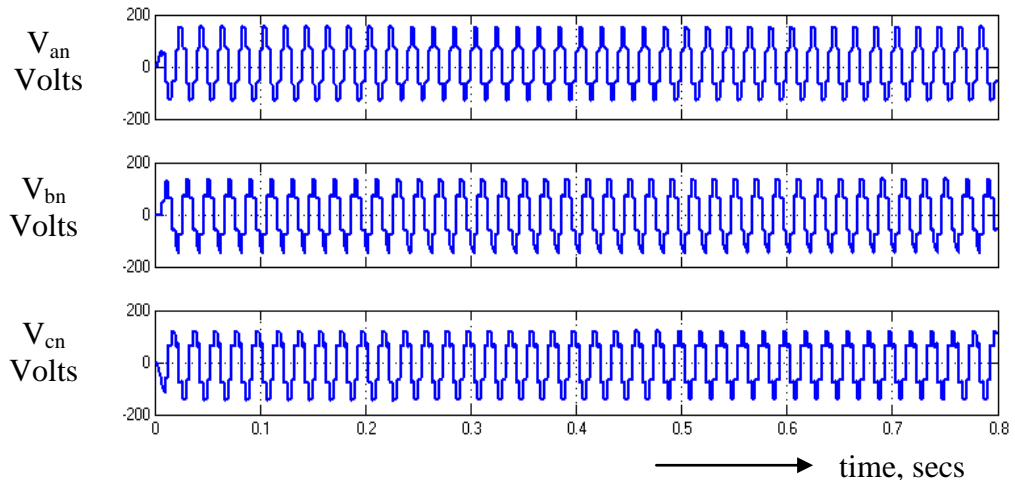


Figure 21. Voltage waveforms of Inverter

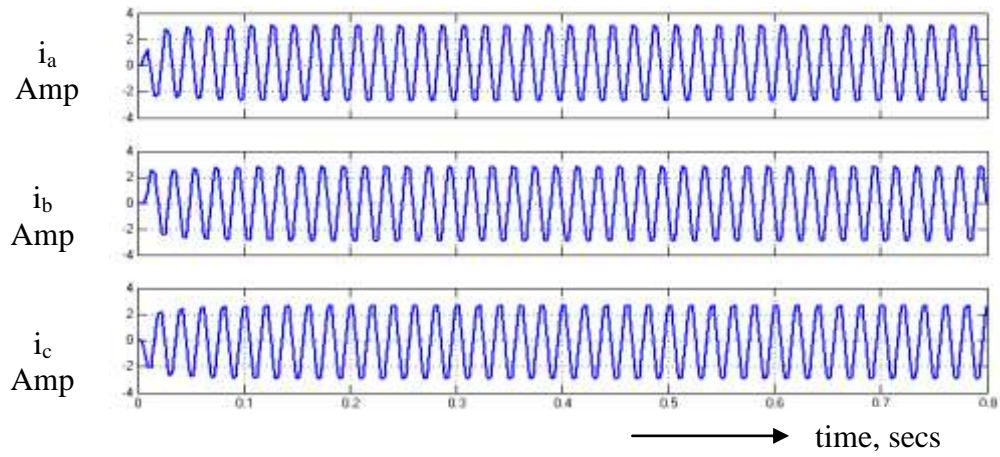


Figure 22. Load current waveforms

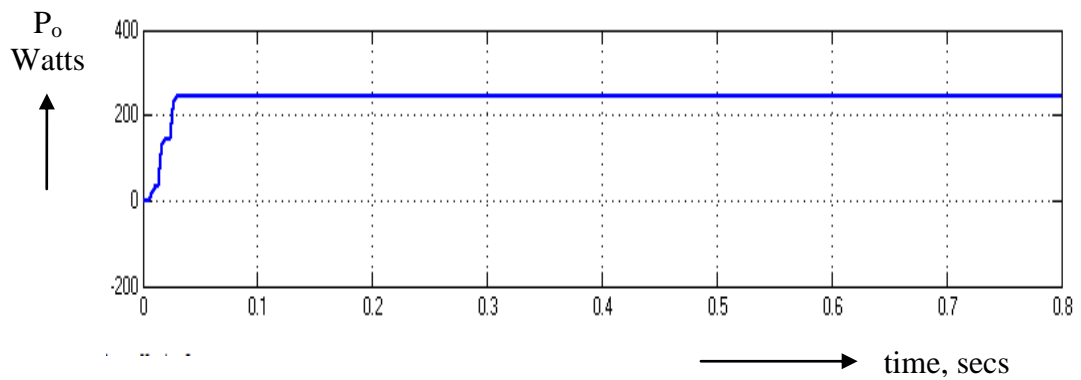


Figure 23. Output power

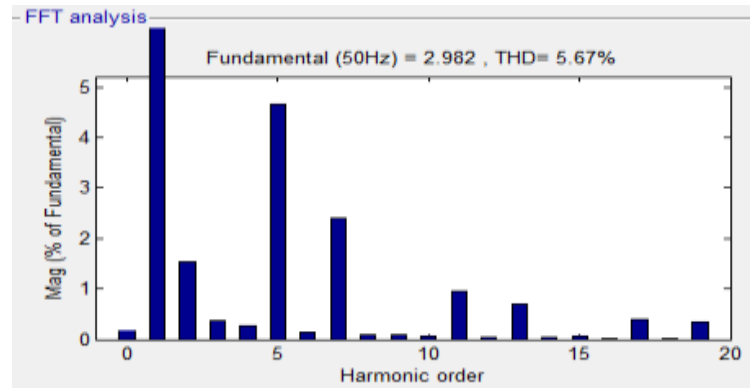


Figure 24. Frequency Spectrum for Current

The summary of time domain parameters using PI and FLC is given in Table 1. It is observed that the settling time and its deviation from the set value are very much reduced using FLC. The summary of output power and THD is given in Table 2. The FLC incorporated closed gives required power and lower THD in the load current. The settling time is reduced from 0.3 to 0.02 seconds and the steady state error is reduced from 2.8V to 0.7V. The THD in FLC based BBCIS system is reduced to 5.67%.

Table 1. Time domain parameters

Controller	Rise time (s)	Peak time (s)	Setting time (s)	Steady state error (Volts)
PI	0.05	0.23	0.3	2.8
FLC	0.01	0	0.02	0.7

Table 2. Comparison of Power & THD

Control	Po	THD
Without MPPT	190w	10%
With MPPT PI	230w	8.14%
With MPPT & Fuzzy	230w	5.67%

4. EXPERIMENTAL RESULTS

The hardware is engineered and tested in the Department. The specifications for the hardware used are given in Table 3.

Table 3. Hardware specifications

Component	Specification
N-channel MOSFET	IRF 840
Current rating	8A
Voltage	500V
Gate voltage	10V
Diode	1N4007
Controller	PIC16F84A
Driver	IR2110
Transformer	230/0-15V 50Hz
Regulator	LM7812
Regulator	LM7805

The hardware snapshot for the CFLI system is reported in Figure 25. The hardware consists of control board, MLI board and driver board. The DC input voltage reported in Figure 26. Driving pulses for S1 and S5 are reported in Figures 27 and 28 respectively. The output of MLI for line to neutral voltage is

reported in Figure 29. The output of line to line voltage is reported in Figure 30. The output voltage has five levels.

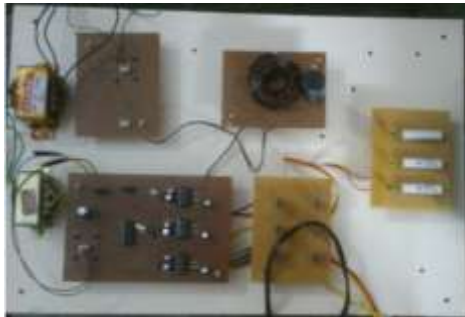


Figure 25. Hardware Snapshot



Figure 26. Output Voltage of Boost Converter (60V)



Figure 27. Driver output pulse S1



Figure 28. Driver output pulse S5

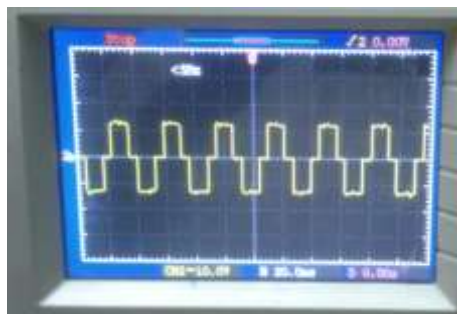


Figure 29. Line to Neutral voltage

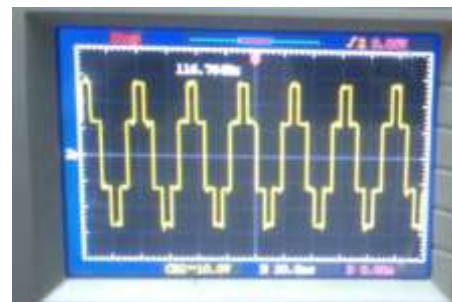


Figure 30. Line Voltage

5. CONCLUSION

Closed loop BBCIS with PI and FLC were modeled and simulated successfully using simulink. The hardware is developed and tested in the laboratory. The investigation indicated that fuzzy logic controlled BBCI system gives rated power with 5.6% of THD. The output power is maintained at 190W using MPPT. The proposed controller sustains constant output power with reduced harmonic content. The analysis and simulation showed that constant real power can be maintained by using FLC. The advantages of proposed system were high voltage gain, low THD and reduced hardware. The disadvantage is that the proposed system requires two boost converters and FLC. The present work deals with comparison of responses of BBCIS with PI and FL controllers. The comparison between PI and ANN will be done in the near future.

REFERENCES

- [1] R. Gonzalez, E. Gubia, J. Lopez, and L. Marroyo, "Transformerless singlephase multilevel-based photovoltaic inverter", *IEEE Trans. Ind. Electron.*, vol. 55, no. 7, pp. 2694–2702, Jul. 2008.
- [2] T. Kerekes, R. Teodorescu, P. Rodriguez, G. Vazquez, and E. Aldabas, "A new high-efficiency single-phase transformerless PV inverter topology", *IEEE Trans. Ind. Electron.*, vol. 58, no. 1, pp. 184–191, Jan. 2011.
- [3] H. Baeberlin, "Evolution of inverters for grid connected PV-Systems from 1989 to 2000", in *Proc. 17th Eur. Photovoltaic Solar Energy Conf.*, Munich, Germany, Oct. 22–26, 2001, pp. 426–430.
- [4] J. M. Carrasco, L. G. Franquelo, J. T. Bialasiewicz, E. Galvan, R. C. Portillo Guisado, M. A. M. Prats, J. I. Leon, and N. Moreno-Alfonso, "Power-electronic systems for the grid integration of renewable energy sources: A survey", *IEEE Trans. Ind. Electron.*, vol. 53, no. 4, pp. 1002–1016, Jun. 2006.
- [5] D. G. Infield, P. Onions, A. D. Simmons, and G. A. Smith, "Power quality from multiple grid-connected single-phase inverters", *IEEE Trans. Power Del.*, vol. 19, no. 4, pp. 1983–1989, Oct. 2004.
- [6] S. B. Kjaer, J. K. Pedersen, and F. Blaabjerg, "A review of single-phase grid-connected inverters for photovoltaic modules", *IEEE Trans. Ind. Appl.*, vol. 41, no. 5, pp. 1292–1306, Sep. 2005.
- [7] W. M. Blewitt, D. J. Atkinson, J. Kelly, and R. A. Lakin, "Approach to low-cost prevention of DC injection in transformerless grid connected inverters", *IET Power Electron.*, vol. 3, no. 1, pp. 111–119, Jan. 2010.
- [8] V. Salas, E. Olías, M. Alonso, F. Chenlo, and A. Barrado, "DC current injection into the network from PV grid inverters", in *Proc. IEEE Photovoltaic Energy Convers. Conf.*, Waikoloa, HI, USA, May 2006, pp. 2371–2374.
- [9] AS 4777.2, Grid connection of energy system via inverters. Part 2: Inverter requirements Australia, 2002.
- [10] "IEEE recommended practice for utility interface of photovoltaic (PV) systems", *IEEE Standard 929-2000*, Apr. 3, 2000.
- [11] ER G83/1, "Recommendations for the connection of small-scale embedded generators (up to 16 A per phase) in parallel with public low-voltage distribution networks", *Eng. Recommendation*, U.K., Sep. 2003.
- [12] R. Gonzalez, J. L. Lopez, P. Sanchis, and L. Marroyo, "Transformerless inverter for single-phase photovoltaic systems", *IEEE Trans. Power Electron.*, vol. 22, no. 2, pp. 693–697, Mar. 2007.
- [13] N. Mohan, T. Undeland, and W. Robbins, *Power Electronics: Converters, Applications and Design*. New York, NY, USA: Wiley, 2002.
- [14] M. Armstrong, D. J. Atkinson, C. M. Johnson, and T. D. Abeyasekera, "Auto-calibrating DC link current sensing technique for transformerless, grid connected, H-Bridge inverter systems", *IEEE Trans. Power Electron.*, vol. 21, no. 5, pp. 1385–1393, Sep. 2006.
- [15] L. Bowtell and A. Ahfock, "Direct current offset controller for transformerless single-phase photovoltaic grid-connected inverters", *IET Renew. Power Gener.*, vol. 4, no. 5, pp. 428–437, Sep. 2010.
- [16] G. Buticchi, E. Lorenzani, and G. Franceschini, "A DC offset current compensation strategy in transformerless grid-connected power converters", *IEEE Trans. Power Del.*, vol. 26, no. 4, pp. 2743–2751, Oct. 2011.
- [17] G. He and D. Xu, "A novel DC loop current control strategy for paralleled UPS inverter system based on decoupled control scheme", in *Proc. Int. Symp. Ind. Electron.*, Hangzhou, China, May 28–31, 2012, pp. 70–75.
- [18] K. Masoud and G. Ledwich, "Grid connection without mains transformers", *J. Electr. Electron. Eng.*, vol. 19, no. 1/2, pp. 31–36, 1999.
- [19] T. Ahfock and L. Bowtell, "DC offset elimination in a single-phase gridconnected photovoltaic system", *Australasian Universities Power Engineering Conference*, Melbourne, Australia, Dec. 10–13, 2006.